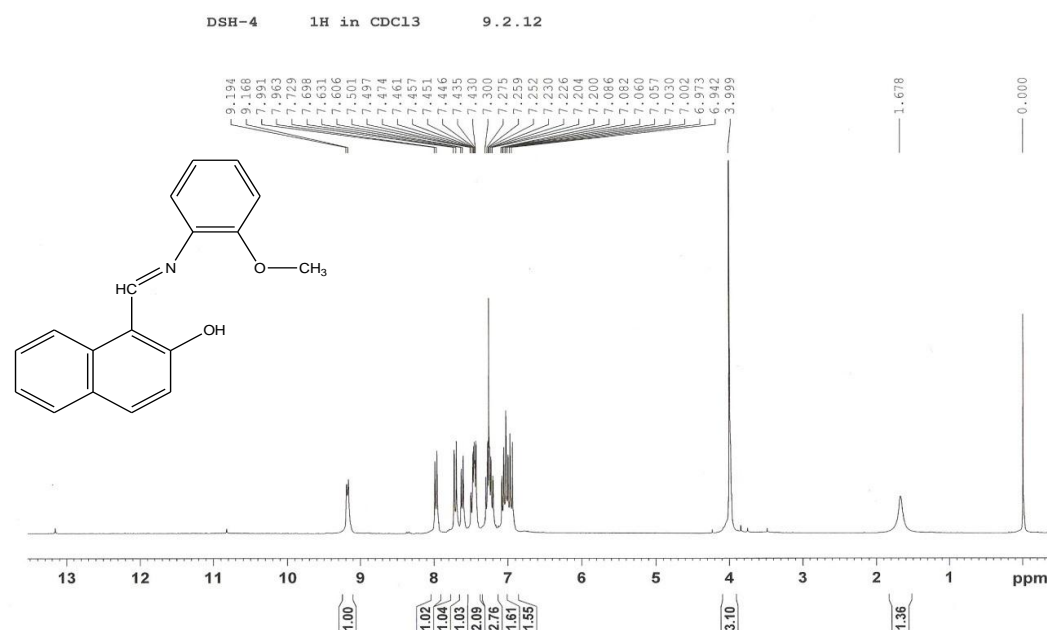


## Supporting Information (ESI)<sup>†</sup>

### Interaction of a naphthalene based fluorescent probe with Al<sup>3+</sup>: Experimental and computational studies.

Sudipta Das, Debasis Karak, Sisir Lohar, Arnab Banerjee, Animesh Sahana and Debasis Das<sup>\*</sup>

Department of Chemistry, The University of Burdwan, Burdwan, West Bengal, India



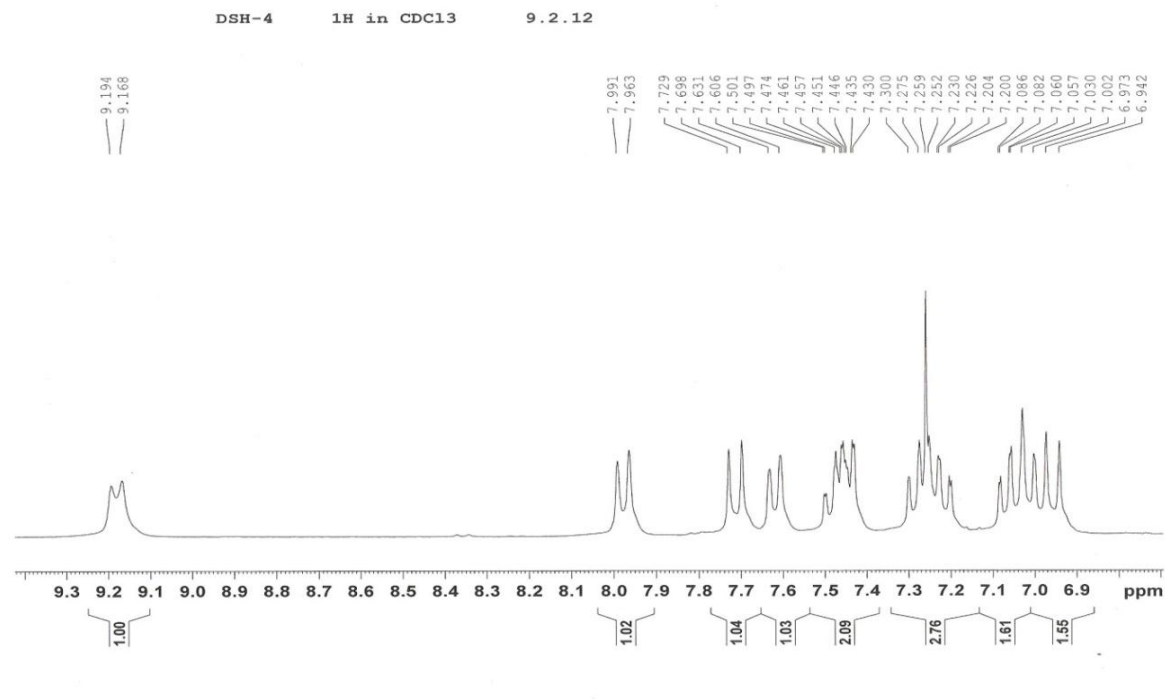


**Fig. S1(b).**  $^1\text{H}$  NMR spectrum (expanded to aromatic region) of **L** in  $\text{CDCl}_3$

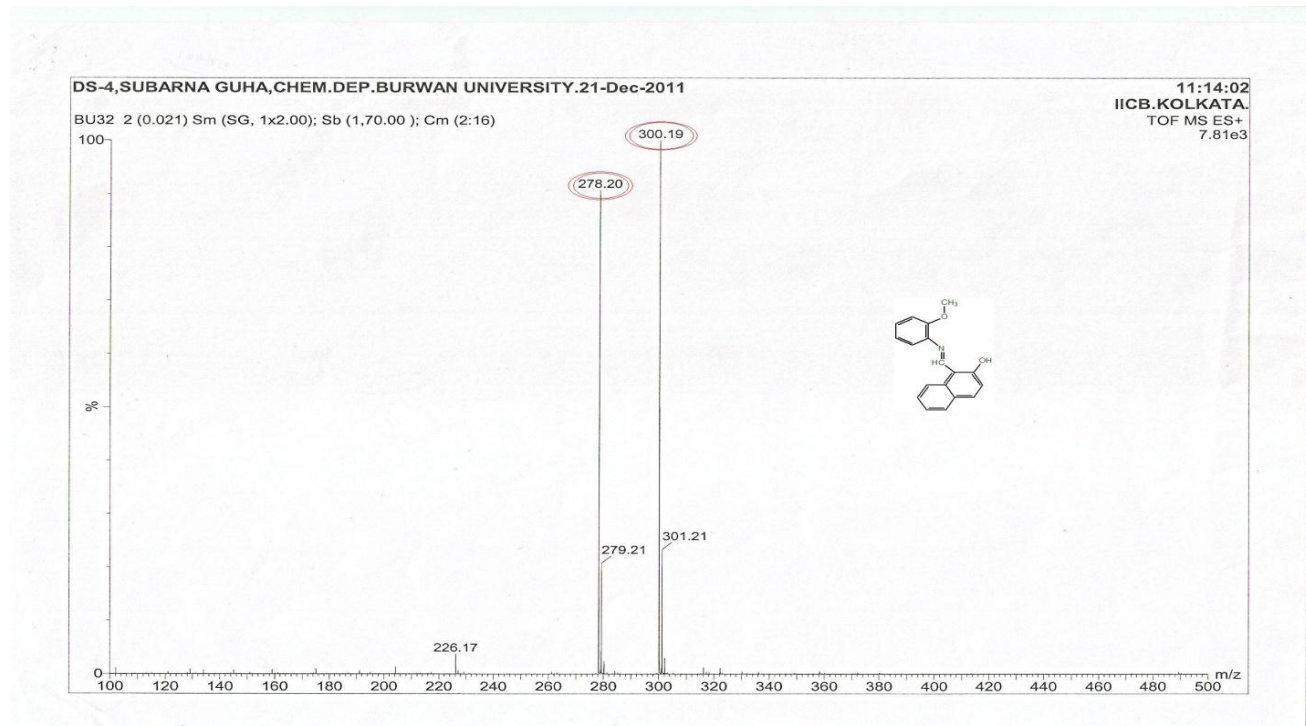


**Fig.S2.** Mass spectra of **L** [ $\text{m/z } [\text{M}+\text{H}]^+ = 278.20$  (92%);  $[\text{M}+\text{Na}]^+ = 300.19$  (100%)]

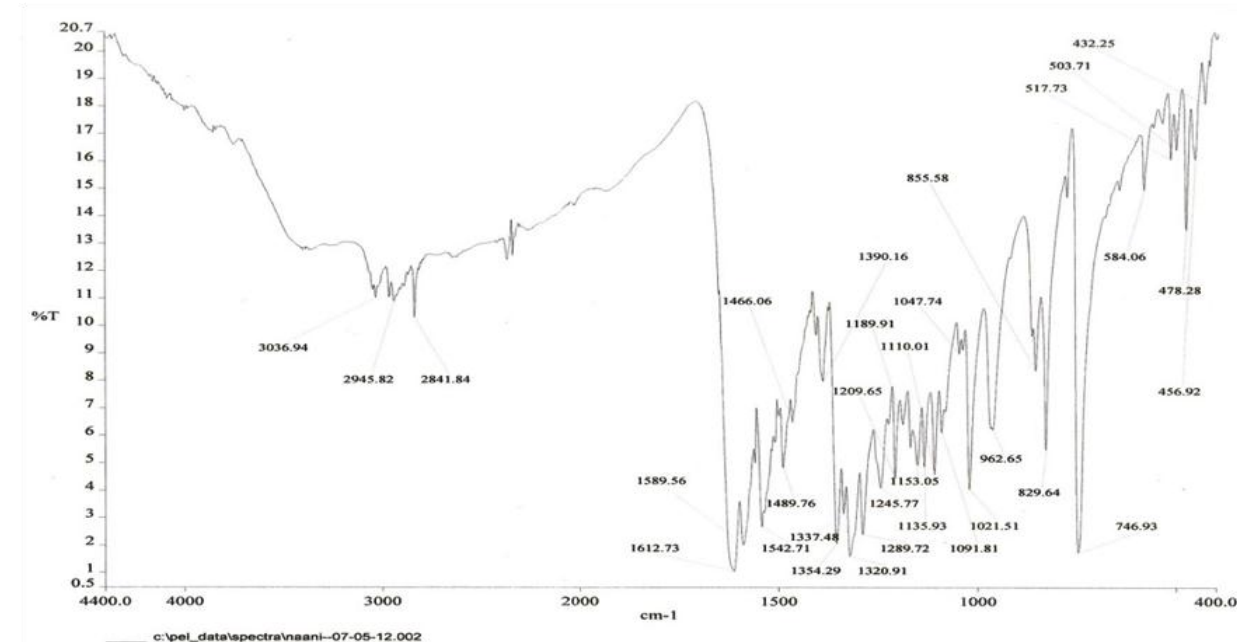


**Fig.S3.** FTIR spectrum of **L**

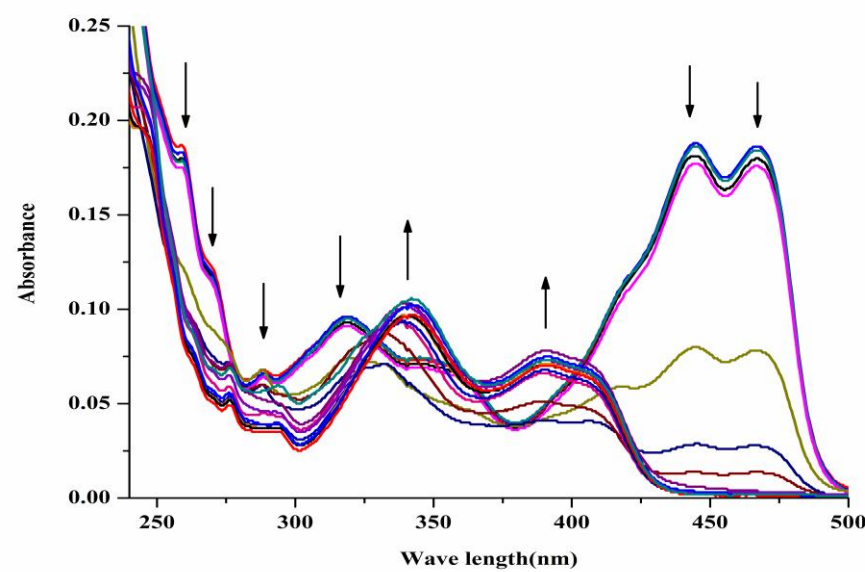


**Fig . S4.** UV-Vis spectral changes of **L** ( $10 \mu M$  in HEPES buffer,  $0.1 M$ , pH 7.4) with gradual addition of 0.5 to 10 times of  $[Al^{3+}]$  (from top to bottom). Two new peaks developed at 392 nm and 340 nm, indicate binding of  $Al^{3+}$  by the **L**.

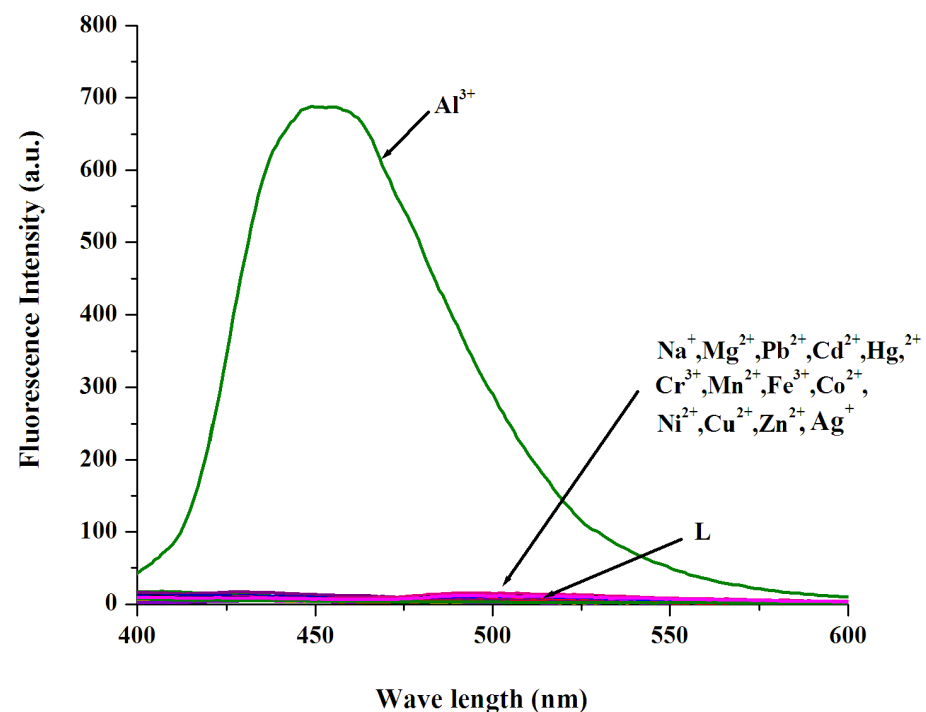


**Fig. S5.** Fluorescence spectra of **L** (10  $\mu\text{M}$ ), **L** + Al<sup>3+</sup> (80  $\mu\text{M}$ ) and **L** (10  $\mu\text{M}$ ) + M<sup>n+</sup> (300  $\mu\text{M}$ ), where M<sup>n+</sup> = Na<sup>+</sup>, Mg<sup>2+</sup>, Cr<sup>3+</sup>, Mn<sup>2+</sup>, Fe<sup>3+</sup>, Co<sup>2+</sup>, Ni<sup>2+</sup>, Cu<sup>2+</sup>, Zn<sup>2+</sup>, Hg<sup>2+</sup>, Pb<sup>2+</sup>, Cd<sup>2+</sup>, Ag<sup>+</sup> ( $\lambda_{\text{em}}$ : 449 nm,  $\lambda_{\text{ex}}$ : 345 nm).

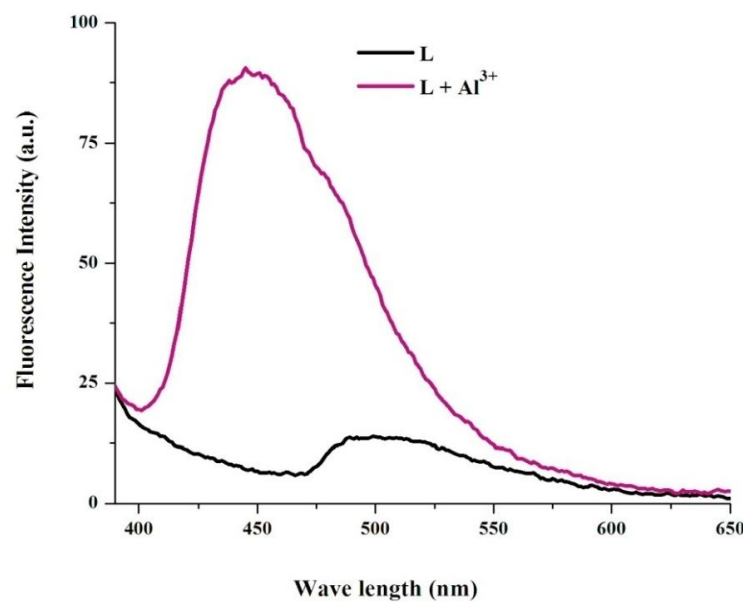


**Fig.S6.** Fluorescence spectra of **L** and its Al<sup>3+</sup> complex ( $\lambda_{\text{ex}} = 345$  nm,  $\lambda_{\text{em}} = 449$  nm).

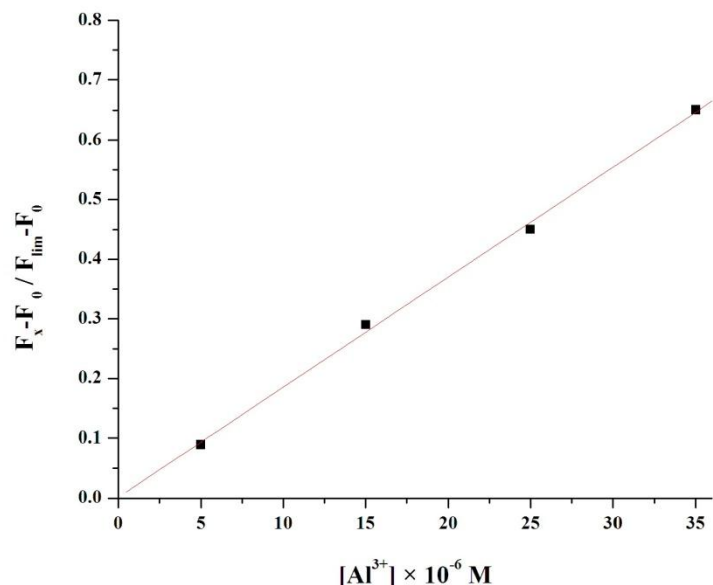


**Fig. S7.** Eission intensities of **L** (10  $\mu\text{M}$ ) as a function of externally added  $[\text{Al}^{3+}]$  in aqueous – methanol ( $\lambda_{\text{em}}$ : 449 nm,  $\lambda_{\text{ex}}$ : 345 nm). The detection limit is  $4.8 \times 10^{-7} \text{ M}$ .

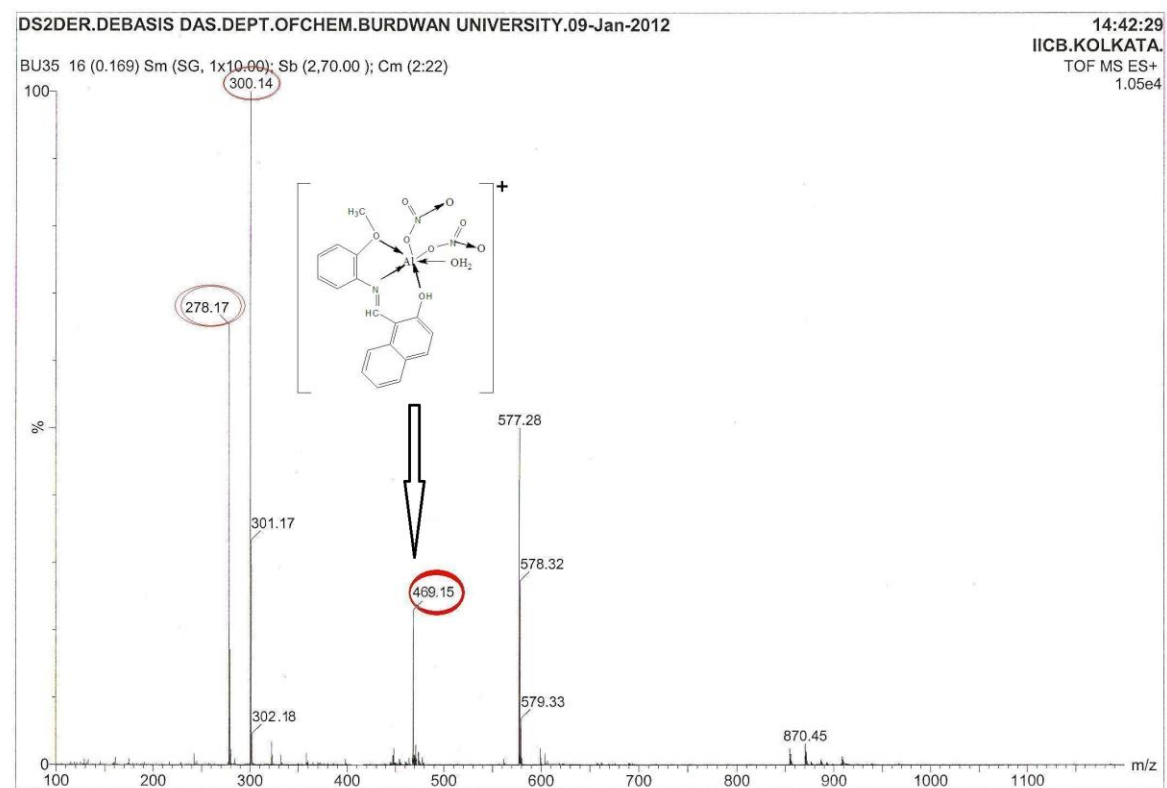


**Fig .S8.** Mass spectra of  $[(\text{L}) \text{Al}(\text{NO}_3)_2(\text{H}_2\text{O})]$  complex

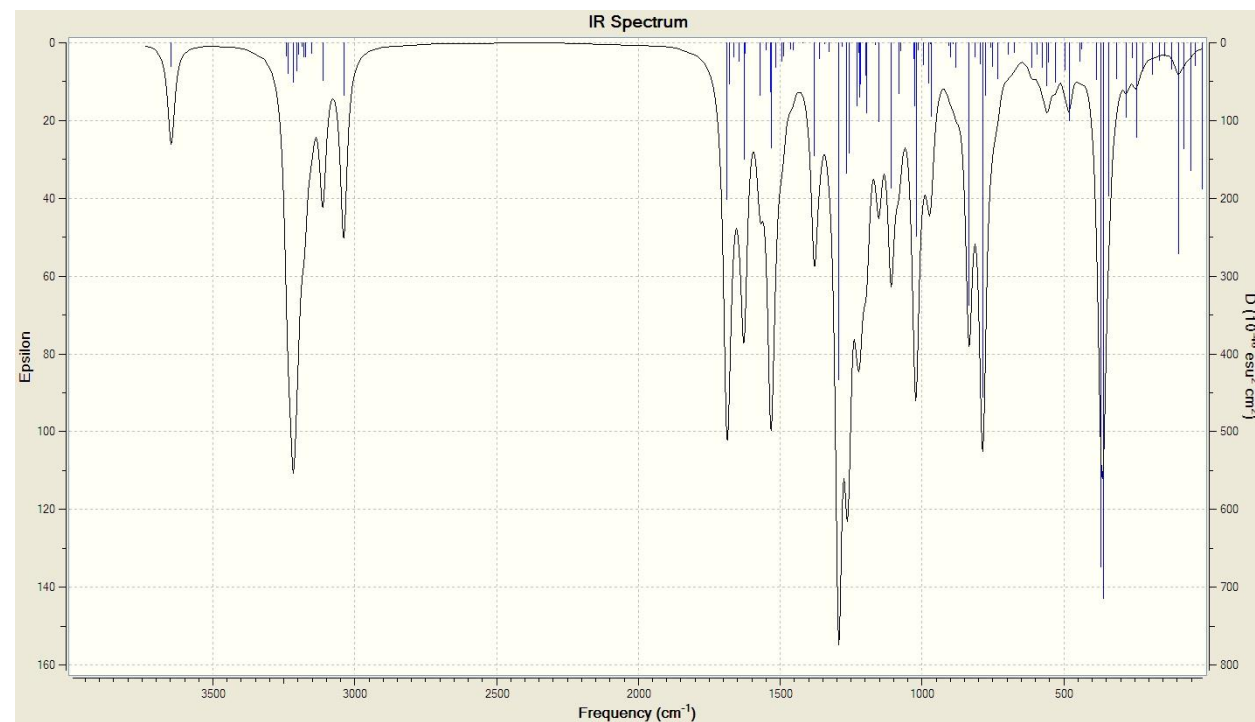


**Fig . S9.** Theoretical IR spectrum of L.

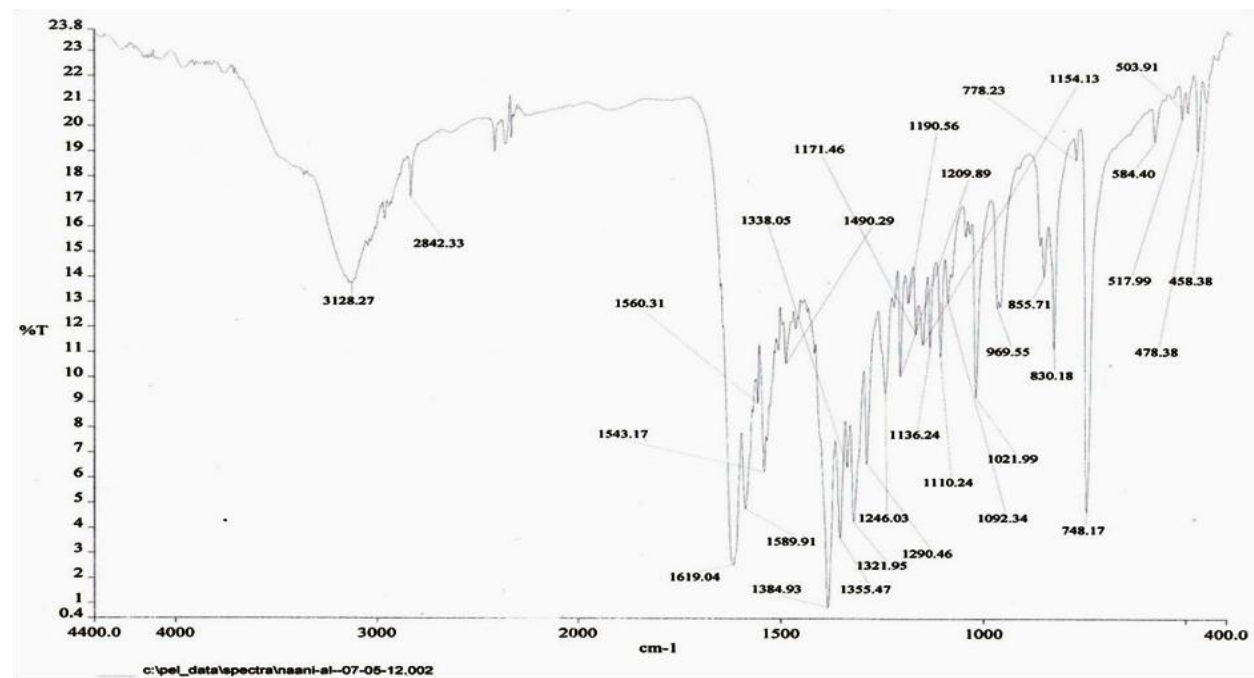


**Fig.S10.** Experimental IR spectrum of L-Al<sup>3+</sup> complex

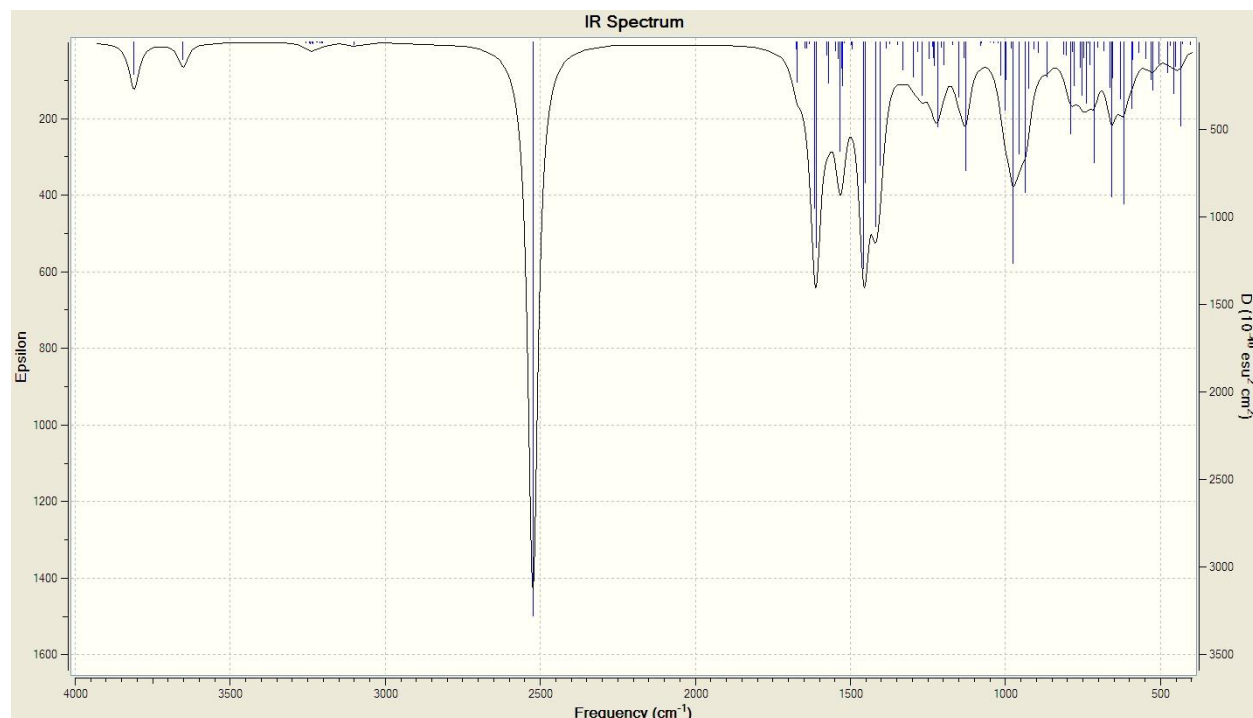


**Fig.S11.** Theoretical IR spectrum of **L-Al<sup>3+</sup>** complex

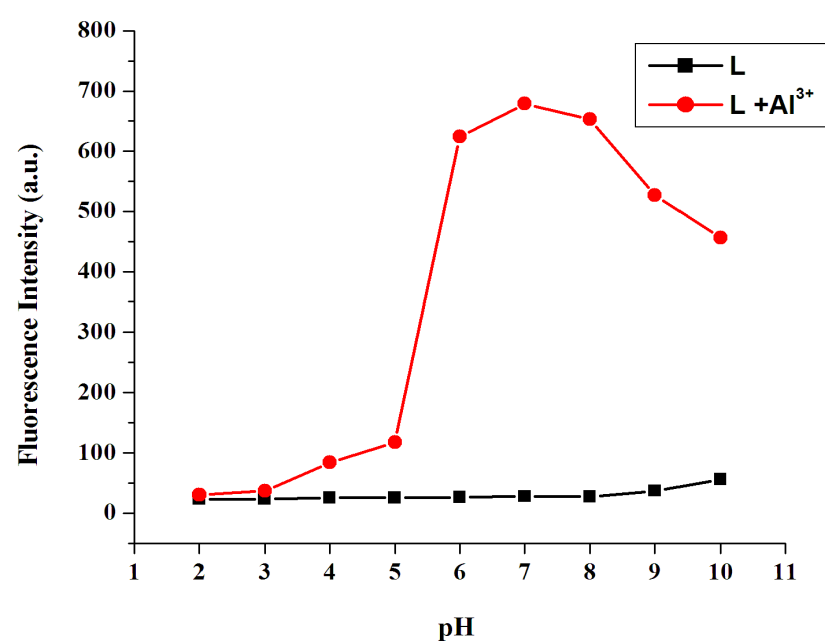
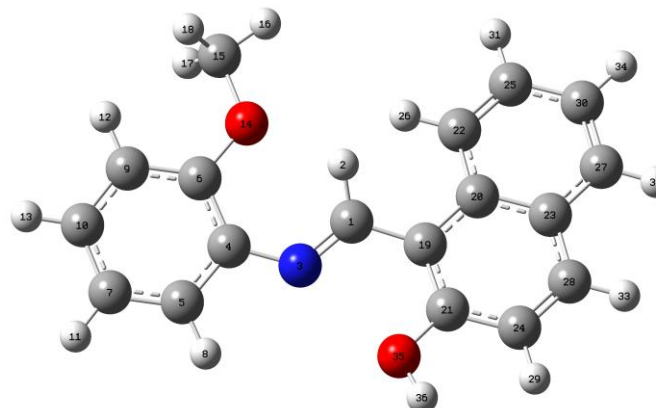


**Fig.S12.** Effect of pH on the binding efficiency of **L** (10 μM) towards Al<sup>3+</sup> (62 × 10<sup>-6</sup> M) in HEPES buffer, 0.1 M, water: methanol = 2:8, v/v) ( $\lambda_{\text{em}}$ : 449 nm,  $\lambda_{\text{ex}}$ : 345 nm).

**Table S1:** Relevant bond lengths and angles of the  $\text{L-Al}^{3+}$  complex (atom numbering refers to Fig. 7 (a) and (b) using the 6-31G basis set.

Bond angle/ $^{\circ}$	Bond angle/ $^{\circ}$	Bond length/ $\text{\AA}$
O (14)-Al (19)-N (3) 81.76	O (47)-Al (19)-O (27) 93.14	Al (19)-O (14)(-OCH <sub>3</sub> ) 1.96
O (47)-Al (19)-N (3) 86.49	O (28)-Al (19)-O (27) 77.70	Al (19)-N (3) (C=N) 1.97
O (14)-Al (19)-O (28) 96.62	O (14)-Al (19)-O (23) 84.54	Al (19)-O (47) (-OH) 1.92
O (28)-Al (19)-O (47) 95.22	O (28)-Al (19)-O (23) 83.97	Al (19)-O (28) (H <sub>2</sub> O) 1.95
O (14)-Al (19)-O (27) 97.14	O (47)-Al (19)-O (23) 88.79	Al (19)-O (23) (NO <sub>3</sub> <sup>-</sup> ) 1.94
N (3)-Al (19)-O(27) 101.63	N (3)-Al (19)-O (23) 96.66	Al(19)-O(27) (NO <sub>3</sub> <sup>-</sup> ) 1.88

**Table: S2.** Natural Population Analysis (NPA) of L .



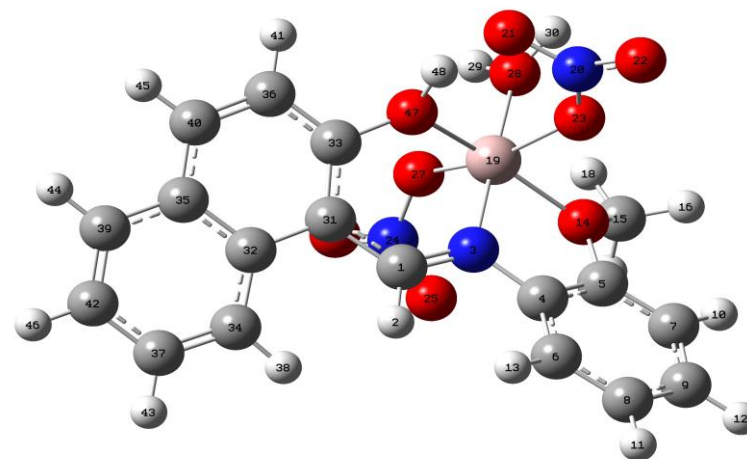
Natural Population Analysis

Atom	No	Charge	Core	Valence	Rydberg	Total
C	1	0.07568	1.99916	3.90775	0.01741	5.92432
H	2	0.21842	0.00000	0.77798	0.00360	0.78158

N	3	-0.42090	1.99924	5.40924	0.01242	7.42090
C	4	0.08654	1.99879	3.89747	0.01721	5.91346
C	5	-0.20642	1.99897	4.19555	0.01191	6.20642
C	6	0.29303	1.99861	3.69318	0.01518	5.70697
C	7	-0.26534	1.99898	4.25514	0.01122	6.26534
H	8	0.26207	0.00000	0.73624	0.00169	0.73793
C	9	-0.32196	1.99895	4.31296	0.01004	6.32196
C	10	-0.22711	1.99900	4.21648	0.01162	6.22711
H	11	0.24429	0.00000	0.75473	0.00098	0.75571
H	12	0.24341	0.00000	0.75548	0.00112	0.75659
H	13	0.24288	0.00000	0.75609	0.00102	0.75712
O	14	-0.53598	1.99972	6.53046	0.00579	8.53598
C	15	-0.35352	1.99927	4.34739	0.00686	6.35352
H	16	0.24188	0.00000	0.75738	0.00075	0.75812
H	17	0.21881	0.00000	0.77879	0.00240	0.78119
H	18	0.21665	0.00000	0.78108	0.00227	0.78335
C	19	-0.11821	1.99885	4.10613	0.01323	6.11821
C	20	-0.02377	1.99894	4.01453	0.01029	6.02377
C	21	0.34475	1.99858	3.64146	0.01520	5.65525
C	22	-0.22869	1.99898	4.21937	0.01034	6.22869
C	23	-0.07375	1.99892	4.06376	0.01106	6.07375
C	24	-0.30426	1.99894	4.29392	0.01140	6.30426
C	25	-0.23196	1.99900	4.22144	0.01152	6.23196
H	26	0.24887	0.00000	0.74936	0.00177	0.75113
C	27	-0.20935	1.99897	4.19971	0.01067	6.20935
C	28	-0.19112	1.99896	4.18133	0.01083	6.19112
H	29	0.23837	0.00000	0.76030	0.00133	0.76163
C	30	-0.24954	1.99899	4.23895	0.01161	6.24954
H	31	0.24247	0.00000	0.75650	0.00103	0.75753
H	32	0.23971	0.00000	0.75900	0.00129	0.76029
H	33	0.24443	0.00000	0.75433	0.00124	0.75557

H	34	0.24377	0.00000	0.75523	0.00100	0.75623
O	35	-0.66738	1.99974	6.66303	0.00462	8.66738
H	36	0.48323	0.00000	0.51498	0.00179	0.51677
<hr/>						
* Total *		0.00000	41.97956	103.75673	0.26371	146.00000

**Table: S3.** Natural Population Analysis (NPA) of L-Al<sup>3+</sup> complex



Natural Population

Atom	No	Charge	Core	Valence	Rydberg	Total
<hr/>						
C	1	0.17120	1.99910	3.81373	0.01596	5.82880
H	2	0.24291	0.00000	0.75541	0.00167	0.75709
N	3	-0.64583	1.99930	5.63112	0.01542	7.64583
C	4	0.10864	1.99874	3.87774	0.01488	5.89136
C	5	0.30963	1.99848	3.67887	0.01301	5.69037
C	6	-0.22959	1.99894	4.22099	0.00966	6.22959
C	7	-0.27621	1.99889	4.26704	0.01028	6.27621
C	8	-0.22227	1.99901	4.21153	0.01172	6.22227
C	9	-0.19689	1.99902	4.18630	0.01158	6.19689

H	10	0.26856	0.00000	0.73052	0.00092	0.73144
H	11	0.27005	0.00000	0.72910	0.00085	0.72995
H	12	0.27059	0.00000	0.72858	0.00083	0.72941
H	13	0.25917	0.00000	0.73982	0.00101	0.74083
O	14	-0.62651	1.99973	6.62117	0.00561	8.62651
C	15	-0.33299	1.99925	4.32702	0.00672	6.33299
H	16	0.24635	0.00000	0.75259	0.00106	0.75365
H	17	0.25905	0.00000	0.73953	0.00141	0.74095
H	18	0.24815	0.00000	0.75049	0.00136	0.75185
Al	19	2.02081	9.99741	0.96905	0.01274	10.97919
N	20	0.69341	1.99963	4.27960	0.02737	6.30659
O	21	-0.46943	1.99982	6.46257	0.00704	8.46943
O	22	-0.25177	1.99979	6.24435	0.00763	8.25177
O	23	-0.65728	1.99982	6.64963	0.00783	8.65728
N	24	0.68135	1.99961	4.28749	0.03154	6.31865
O	25	-0.39963	1.99982	6.39313	0.00668	8.39963
O	26	-0.30136	1.99980	6.29417	0.00739	8.30136
O	27	-0.74290	1.99982	6.73569	0.00739	8.74290
O	28	-1.00720	1.99981	7.00262	0.00477	9.00720
H	29	0.57053	0.00000	0.42779	0.00168	0.42947
H	30	0.55969	0.00000	0.43903	0.00129	0.44031
C	31	-0.15065	1.99882	4.14103	0.01080	6.15065
C	32	-0.00582	1.99895	3.99642	0.01045	6.00582
C	33	0.36445	1.99856	3.62345	0.01355	5.63555
C	34	-0.23449	1.99897	4.22535	0.01017	6.23449
C	35	-0.06703	1.99892	4.05724	0.01087	6.06703
C	36	-0.27971	1.99890	4.26893	0.01189	6.27971
C	37	-0.19086	1.99901	4.18011	0.01174	6.19086
H	38	0.24459	0.00000	0.75421	0.00120	0.75541
C	39	-0.18871	1.99897	4.17870	0.01104	6.18871
C	40	-0.12821	1.99898	4.11858	0.01064	6.12821

H	41	0.27564	0.00000	0.72336	0.00100	0.72436
C	42	-0.22197	1.99899	4.21127	0.01171	6.22197
H	43	0.26454	0.00000	0.73458	0.00089	0.73546
H	44	0.25971	0.00000	0.73917	0.00111	0.74029
H	45	0.26865	0.00000	0.73026	0.00109	0.73135
H	46	0.26672	0.00000	0.73243	0.00085	0.73328
O	47	-0.84858	1.99975	6.84459	0.00424	8.84858
H	48	0.55150	0.00000	0.44466	0.00384	0.44850
<hr/>						
* Total *		1.00000	69.97459	159.65103	0.37439	230.00000

**Table S4.** Theoretical *vs.* experimental IR data of **L** and [**L**+Al<sup>3+</sup>] complex.

System	Theoretical v/ cm <sup>-1</sup>	Experimental v/ cm <sup>-1</sup>
<b>L</b>	352,402,492,585,785,862,948,1026, 1098,1142,1202,1250,1300,1364, 1544,1625,1685,3052,3102,3225, 3650.	456, 478, 584, 746, 829, 855, 962, 1021, 1091,1135,1153,1245,1289,1320,1337, 1354,1489,1542,1589,1612,2841,2945, 3036.
<b>L+ Al<sup>3+</sup></b>	410,584,608,698,742,785,962,1112, 1201,1284,1402,1450,1524,1612, 2024,3242,3648,3801	458,478,517,584,748,778,969,1021, 1092,1171,1110,1136,1190,1209, 1246,1290,1321,1246,1355,1384, 1589, 1560,1619,2842,3128.

### General method of UV-Vis and fluorescence titration

Path length of the cells used for absorption and emission studies was 1 cm. For UV-Vis and fluorescence titrations, stock solution of **L** (10 μM) was prepared in methanol water (2:8, v/v). Working solutions were prepared from their respective stock solutions. Fluorescence measurements were performed using 5 nm × 5 nm slit width.

### Calculation of Quantum Yield

Fluorescence quantum yields ( $\Phi$ ) were estimated by integrating the area under the fluorescence curves using the equation<sup>1</sup>,

Where,  $A$  was the area under the fluorescence spectral curve,  $OD$  was optical density of the compound at the excitation wavelength and  $\eta$  was the refractive indices<sup>2</sup> of the solvent. Anthracene was used as quantum yield standard (quantum yield is 0.27 in ethanol)<sup>3</sup> for measuring the quantum yields at 330 nm.

### References

1. E. Austin and M. Gouterman, *Bioinorg. Chem.*, 1978, 9, 281.
2. F. I. El - Dossoki, *J. Chin. Chem. Soc.* 2007, 54, 1129.
3. W. H. Melhuish, *J. Phys. Chem.*, 1961, 65, 229.